



Cite this: RSC Adv., 2017, 7, 47583

Molecular dynamics simulation for the impact of an electrostatic field and impurity Mg^{2+} ions on hard water

Lin Zhu, ^a Yong Han, ^{*a} Chuanxin Zhang, ^a Ruikuan Zhao^a and Shoufeng Tang^b

A detailed analysis of the structural parameters and dynamic parameters of hard water solutions under an external electrostatic field was performed by molecular dynamics (MD) simulations with the presence of impurity Mg^{2+} ions. The $CaCl_2$ aqueous solution was chosen in the study as hard water because calcium carbonate is the main component of water scale. The effects on the $CaCl_2$ aqueous solution caused by adding different numbers of Mg^{2+} ions and using an electrostatic field are examined in terms of the self-diffusion coefficient of Ca^{2+} ions and water molecules, the residence time of water molecules in the first water shell of Ca^{2+} ions, solution viscosity, characteristics of hydrogen bonds and some structural parameters, and how these effects influence the formation process of calcium carbonate when there are CO_3^{2-} ions. The goal behind the study is to attain additional insights into the influence on the scale-inhibiting performance with the presence of impurity Mg^{2+} ions when electrostatic anti-fouling technology is used practically in hard water.

Received 1st September 2017
 Accepted 27th September 2017

DOI: 10.1039/c7ra09715h

rsc.li/rsc-advances

1 Introduction

The scale issue is a key problem in heat exchangers, such as cooling towers and boilers. Scaling causes at least two problems: degradation in the performance of heat exchangers and a decrease of flow rate or an increase in pressure drop across the heat exchanger. To solve the scale problem, electrostatic anti-fouling (EAF) systems are used. Many researchers have studied the anti-fouling mechanism of the EAF system. Calcium carbonate is the main component of water scale. Therefore, the vast majority of researchers who investigate the anti-fouling mechanism of EAF systems focus on the effect of electromagnetic fields on calcium carbonate. It mainly includes two aspects: the formation process of calcium carbonate crystallization and the change in the crystal structure of scale under an electromagnetic field. Qi *et al.*¹ investigated the effect of an electric field (EF) on the crystallization of calcium carbonate. Their results showed that the lattice structure and crystalline morphology of $CaCO_3$ can be tailored by the electric field applied to the solution during its crystallization. Liu *et al.*² found that the content of aragonite increased in the scale sample formed in electrostatic water.

However, although the composition of scale is mainly calcium carbonate, there is a small amount of precipitation

formed by Mg^{2+} ions, such as magnesium carbonate and magnesium hydroxide, which are produced by Mg^{2+} and exist in natural water at high temperatures. Therefore some researchers have studied the effect of Mg^{2+} ions on the crystal structure of calcium carbonate. Mitsutaka Kitamura³ studied the crystallization and transformation mechanisms of calcium carbonate polymorphs under the effect of Mg^{2+} . The experimental results showed that Mg^{2+} ions can inhibit the growth of calcite and suppress vaterite transformation to calcite. Gutjahr *et al.*⁴ studied the influence of the divalent cation Mg^{2+} on the growth and dissolution rates of calcite and aragonite. The results showed that ions of the transition metals exhibit stronger inhibition than earth alkaline ions, and Mg^{2+} has no influence on the growth and dissolution of aragonite. DeLeeuw⁵ found that the presence of magnesium and iron ions inhibits calcite growth using molecular dynamics simulations. However, the influence on the microcosmic particle structure in aqueous solutions containing impurity ions under an electrostatic field has received less attention.

There are almost no CO_3^{2-} ions in hard water because of the very low solubility of calcium carbonate. But many HCO_3^- ions exist. Ca^{2+} ions exist in aqueous solution as hydrated ions. These hydrated ions are also combined with other water molecules by hydrogen bonding.⁶⁻⁸ The structural and dynamical properties of Ca^{2+} directly affect the formation, growth and crystal structure of calcium carbonate precipitation. Therefore, research to determine the influence of an electrostatic field and Mg^{2+} ions on the structure and dynamics of hydrated Ca^{2+} may help discern the anti-fouling mechanism of EAF technology.⁹⁻¹⁷ In the present study, a mixed solution of calcium chloride and

^aMeasurement Technology and Instrumentation Key Laboratory of Hebei Province, School of Electrical Engineering, Yanshan University, Qinhuangdao 066004, P. R. China. E-mail: hanyong@ysu.edu.cn

^bSchool of Environmental and Chemical Engineering, Yanshan University, Qinhuangdao 066004, P. R. China



magnesium chloride was chosen. The structure and dynamics performance of the CaCl_2 aqueous solution (the viscosity of the CaCl_2 aqueous solution, the location of the first water shell of Ca^{2+} , the structure of the hydrated Ca^{2+} and the self-diffusion coefficient of Ca^{2+} and water molecules, and the hydrogen bonding in solution) under an external electrostatic field with different numbers of Mg^{2+} ions added were studied using MD simulations.

2 Model and simulation details

The MD simulation used in the present study was an equilibrium MD simulation process. All MD simulations in this work were performed using the Gromacs 5.0.2 software.¹⁸ The length of the simulation box is $4 \text{ nm} \times 4 \text{ nm} \times 3 \text{ nm}$. To study the effect of Mg^{2+} on the CaCl_2 aqueous solution system under the electrostatic field, four sets of aqueous solution systems were built as shown in Table 1. The concentration of the CaCl_2 aqueous solution was 4 mol kg^{-1} , and the concentration uncertainties between simulations and experiments were below 0.5%.¹² The SPCE model was adopted for water molecules in our work. The GROMOS force field^{19–21} was used in this simulation for ion–water interactions. For Lennard-Jones interactions, a cut-off was applied at 0.7 nm, while electrostatic interactions were treated with the particle mesh Ewald (PME)²⁰ method and a real space cut-off of 0.7 nm. The value of Fourier spacing is 0.12 nm. Table 2 presents the Lennard-Jones potential parameters for particles used in the GROMOS force field. The time step used for all the simulations was 2.0 fs. The simulation time was $2.5 \times 10^4 \text{ ps}$. Averages of parameters (except the data of the self-diffusion coefficient) were obtained from the last $1.5 \times 10^4 \text{ ps}$ of every simulation and the averages of parameters were obtained by calculating the average value of $1.5 \times 10^4 \text{ ps}$, which was divided into ten segments. The type of integration algorithm for the equations of motion is the Leap frog algorithm. The temperature was set at 300 K. The pressure was set at $1.01 \times 10^5 \text{ Pa}$. All simulations were carried out in NPT ensembles.

The study consists of two parts. In the first part, a different number of Mg^{2+} ions was added to the CaCl_2 aqueous solution compared to the condition of no Mg^{2+} ions added. In the second part, an external electrostatic field was added compared to the condition of no electrostatic field. The electrostatic field had an intensity of $1 \text{ V } \mu\text{m}^{-1}$. The electrostatic field was applied along a given direction (corresponding to the y-axis). The correctness

Table 1 Composition of the calcium chloride solution studied by Gromacs^a

Sample	[H_2O]	[Mg^{2+}]	[Ca^{2+}]	[Cl^-]	[Total]
0M	1110	0	80	160	1350
1M	1110	10	80	180	1380
2M	1110	20	80	200	1410
3M	1110	30	80	220	1440

^a Note: “0M” means no Mg^{2+} ions are added, “1M” means 10 Mg^{2+} ions are added, “2M” means 20 Mg^{2+} ions are added and “3M” means 30 Mg^{2+} ions are added.

Table 2 Lennard-Jones potential parameters used in the MD simulations. According to Lorentz and Berthelot combining rules, i.e. $\varepsilon_{ij} = (\varepsilon_{ii}\varepsilon_{jj})^{1/2}$ and $\sigma_{ij} = (\sigma_{ii} + \sigma_{jj})/2$

	$\varepsilon/(\text{kJ mol}^{-1})$	σ/nm
Ca^{2+}	0.5069	0.2813
Mg^{2+}	0.3126	0.1933
Cl^-	1.2889	0.3470
O	1.7250	0.2626

of our MD simulations and error analysis has been verified in previous work.²²

3 Results and discussion

3.1 Self-diffusion coefficients of Ca^{2+} ions and water molecules

In this section the self-diffusion coefficients of Ca^{2+} and water molecules were studied when there is an external electrostatic field and a small number of Mg^{2+} ions in the CaCl_2 aqueous solution system. The self-diffusion coefficient of ions is an important parameter which can influence the chemical reaction process in aqueous solution systems. In addition, the self-diffusion coefficient can vary significantly when the structure of the cation or anion changes or when some other kind of ion gets involved.²³

In this paper, the self-diffusion coefficients of Ca^{2+} (D_{Ca}) and water molecules (D_{o}) are calculated based on the “Einstein relation”:²⁴

$$D = \lim_{t \rightarrow \infty} \frac{1}{6t} \left\langle [r_i(t) - r_i(0)]^2 \right\rangle \quad (1)$$

where $r_i(t)$ is the molecule position i at time t , hence $r_i(0)$ is the initial position and the bracket represents the ensemble average. A specific step in calculating the self-diffusion coefficient of particles is to fit the slope of the linear portion of the mean square displacement (MSD) and to divide by 6. The linear portion of the MSD is determined by the RANSAC algorithm. RANSAC is an algorithm for the robust fitting of models in the presence of data outliers.²⁵

Fig. 1 shows the effect of Mg^{2+} on the self-diffusion coefficients of Ca^{2+} and water molecules under an electrostatic field and with no electrostatic field. The standard deviations of the simulation data presented in Fig. 1 are conservatively estimated to be in the range of $0.0046\% \times 10^{-5}$ – $0.0078\% \times 10^{-5} \text{ cm}^2 \text{ s}^{-1}$ for self-diffusion coefficients. According to Fig. 1, the diffusion coefficients of Ca^{2+} and water molecules both decrease with the addition of Mg^{2+} whether there is an electrostatic field or not. Moreover, the more Mg^{2+} ions added, the lower the self-diffusion coefficients of Ca^{2+} and water molecules are. Under no electrostatic field, when ten Mg^{2+} ions are added, D_{o} and D_{Ca} have maximum values of $0.5505 \times 10^{-5} \text{ cm}^2 \text{ s}^{-1}$ and $0.0570 \times 10^{-5} \text{ cm}^2 \text{ s}^{-1}$, respectively. When thirty Mg^{2+} ions are added, D_{o} and D_{Ca} have a minimum value of $0.3223 \times 10^{-5} \text{ cm}^2 \text{ s}^{-1}$ and $0.0250 \times 10^{-5} \text{ cm}^2 \text{ s}^{-1}$, respectively. In addition, Fig. 1(a) shows that the external electrostatic field can make the self-diffusion coefficient of water molecules larger no matter how many

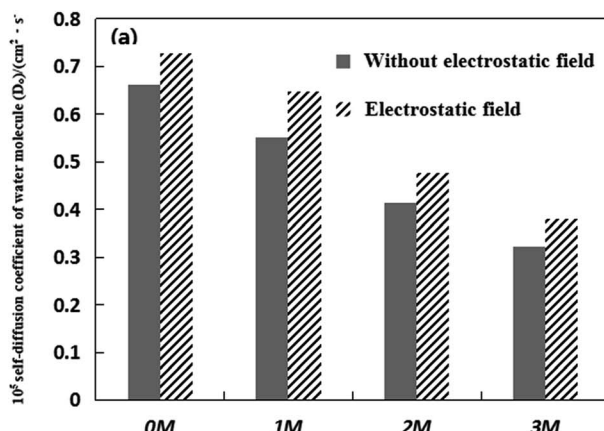


Fig. 1 10^5 self-diffusion coefficient of water molecules (D_o) and Ca^{2+} (D_{Ca}) with no Mg^{2+} ions added (0M), ten Mg^{2+} ions added (1M), twenty Mg^{2+} ions added (2M) and thirty Mg^{2+} ions added (3M) under no electrostatic field and under an electrostatic field.

Mg^{2+} ions are added to the CaCl_2 aqueous solution in all simulations. According to Fig. 1(b), the external electrostatic field can make the self-diffusion coefficient of Ca^{2+} larger without Mg^{2+} addition, which is consistent with the results of our previous study.²⁶ However, the electrostatic field can make the self-diffusion coefficient of Ca^{2+} smaller when Mg^{2+} ions are added to the CaCl_2 aqueous solutions, which means that the combination of impurity Mg^{2+} and of an external electrostatic field can limit the activity of Ca^{2+} more strongly.

In the aqueous solution system, the valence state and structural order of cations can influence the diffusivity of water molecules.²⁷ Mg^{2+} ions lose two electrons and, hence, have a strong binding ability towards water molecules. The first water shell of Mg^{2+} , which consists of six water molecules, has octahedral symmetry. The stability of the nearest shell surrounding the Mg^{2+} ions justifies the assumption that the ion and its first shell can be considered as a solute.^{28,29} To sum up, when Mg^{2+} ions are added to the CaCl_2 solution, the strong ability of Mg^{2+} to bind water molecules makes the activity of water molecules more limited.³⁰ The self-diffusion coefficient of water molecules decreases. And the more Mg^{2+} ions added, the more limited the activity of the water molecules is. The reduction of the self-diffusion coefficient of Ca^{2+} can be attributed to the presence of Mg^{2+} . The electrostatic interaction between Mg^{2+} and water molecules makes the CaCl_2 aqueous solution more compact, which limits the activity of Ca^{2+} , and hence reduces the self-diffusion coefficient of Ca^{2+} .

When the electrostatic field is applied to the pure water solution, the order of the water molecules and the strength of the hydrogen bonds are enhanced, which decrease the self-diffusion coefficient of the water molecules.³¹ It means that the electrostatic field strengthens the correlation ability of the

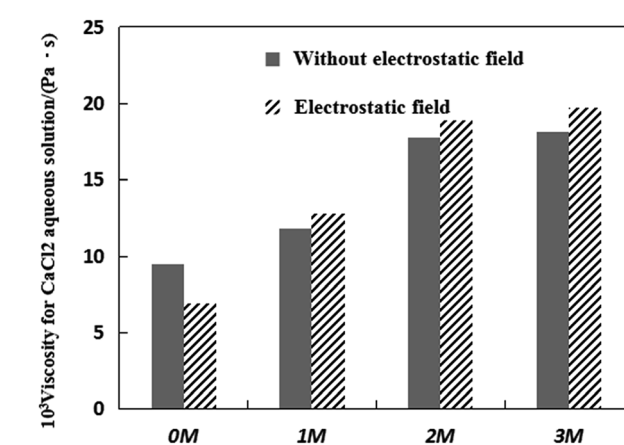
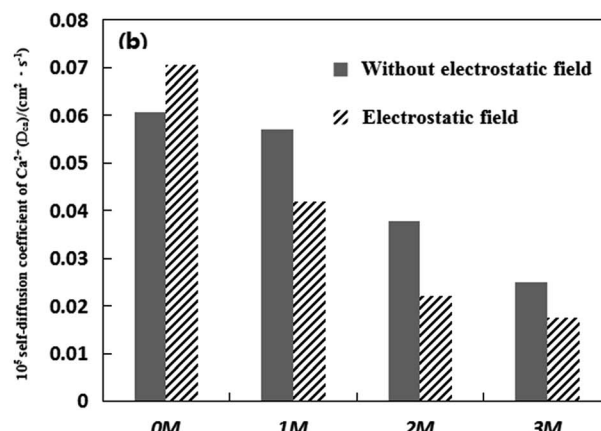


Fig. 2 10^3 average viscosity with no Mg^{2+} ions added (0M), ten Mg^{2+} ions added (1M), twenty Mg^{2+} ions added (2M) and thirty Mg^{2+} ions added (3M) under no electrostatic field and under an electrostatic field.

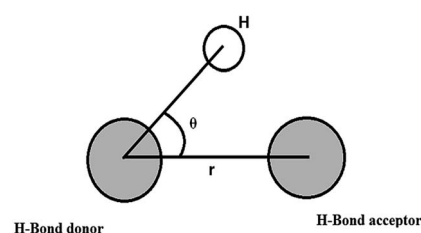


Fig. 3 Geometrical hydrogen bond criterion.

water molecules and the hydrogen bond network in a pure water solution. However, the results in Fig. 1(a) show that the electrostatic field can make the self-diffusion coefficient of water

Table 3 The mean dynamical residence time of water around Ca^{2+} (ps) in the four CaCl_2 solutions

Without an electrostatic field				Under an electrostatic field				
0M	1M	2M	3M	0M	1M	2M	3M	
τ_{res} (ps)	3.7123	3.7503	4.4396	5.9746	3.5893	3.6639	4.1182	5.2266

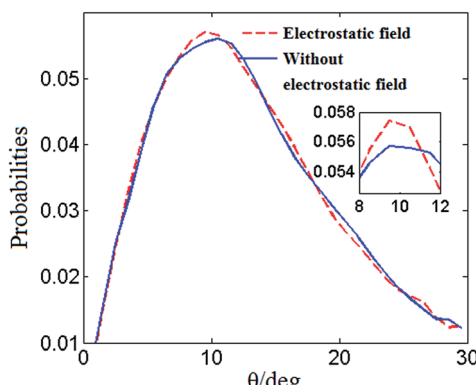


Fig. 4 Distribution of the hydrogen bond angle θ without an electrostatic field (solid line) and with an electrostatic field (dashed line).

molecules larger for the four representative CaCl_2 aqueous solutions. Therefore, the increase of the diffusion coefficient of water molecules in the CaCl_2 aqueous solution should be due to the activity of existing metal ions. The increase of the self-diffusion coefficient of water molecules illustrates that the electrostatic field increases the ionic motion and influences the relatively stable water molecules' hydrogen bond network.

The electrostatic field can not only reduce the diffusion coefficient of Ca^{2+} but also increase the diffusion coefficient of water molecules in the CaCl_2 aqueous solution when the Mg^{2+} ions are added. The less active the Ca^{2+} ions, the smaller the chance of the chemical reaction produced by the combination of Ca^{2+} and CO_3^{2-} is. As the self-diffusion coefficients of Ca^{2+} ions decrease, less CaCO_3 precipitate is generated in solution. Therefore, the application of an electrostatic field with the addition of Mg^{2+} ions is beneficial to scale inhibition, which is consistent with some researchers' work, who have pointed out the inhibition effect of Mg^{2+} on calcium carbonate under an electrostatic field.⁵ Then the scale problem is alleviated.

3.2 Dynamical residence time

The residence time is another important parameter related to the dynamic structure of the solution.³² The residence time

describes the stability of the water molecules, and is related to the strength of hydration.³³ Dynamical residence time γ_{res} is defined as how long an atom or ion stays in a certain shell of another atom or ion.¹² In the present paper the dynamical residence time of water molecules in the first hydration shell of Ca^{2+} was studied to investigate the translational dynamics of the water molecule. The dynamical residence time was calculated using eqn (2):³⁴

$$\gamma = \frac{1}{N_h} \sum_{i=1}^{N_h} \gamma_i \quad (2)$$

where N_h is the hydration number of the shell, and γ_i is the residence time of the water molecule i , which is calculated with eqn (3):

$$\gamma_i = \frac{t_i}{n_i} \quad (3)$$

where t_i is the total time length (picoseconds, ps) of water molecules i staying at the layer assigned, and n_i is the number of times water molecules i leave and come back to the layer assigned.

Table 3 shows the mean dynamical residence time of water around Ca^{2+} in four representative CaCl_2 aqueous solutions under the electrostatic field. The values of γ_{res} under no electrostatic field have been presented for comparison. The standard deviation of γ_{res} is between 0.0086 ps and 0.0095 ps. According to Table 3, under the electrostatic field the mean dynamical residence time of water molecules around Ca^{2+} decreased. In addition, it can be found that the mean dynamical residence time of water around Ca^{2+} rises with the increase in the number of Mg^{2+} ions added in CaCl_2 systems whether the electrostatic field is applied or not.

Naor *et al.*³⁵ studied Ca^{2+} in liquid water using the Car–Parinello molecular dynamics simulation finding that the γ_{res} is 10 ps. Schwenk *et al.*³⁶ studied the dynamics of the solvation process of Ca^{2+} in water based on DFT/MM and QM/MM-HF simulations and the results showed that γ_{res} is 1.2 ps and 2 ps, respectively. According to Table 3, the values of γ_{res} are distributed in the range of 3 to 5 ps, which are similar to the results given in the literature. The increase in the mean

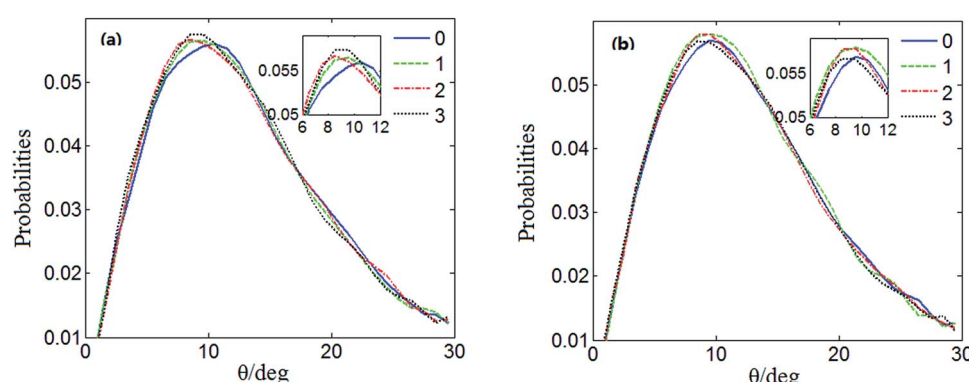


Fig. 5 Distribution of the hydrogen bond angle θ with no Mg^{2+} ions added (solid line), ten Mg^{2+} ions added (dashed line), twenty Mg^{2+} ions added (dash-dotted line) and thirty Mg^{2+} ions added (dotted line). (a) is under no electrostatic field and (b) is under an electrostatic field.



Table 4 The percentage of water molecules with n hydrogen bonds (f_n), the number of Mg^{2+} ions added is $M(n \times 10M)$, the average number of hydrogen bonds in water molecules (n_{HB}) and the average lifetime of hydrogen bonds (τ)

	Without an electrostatic field				Under an electrostatic field			
	0M	1M	2M	3M	0M	1M	2M	3M
f_0 (%)	58.09	60.85	62.41	64.49	57.99	60.12	62.10	64.00
f_1 (%)	31.17	29.36	28.25	28.19	31.08	29.44	28.52	28.39
f_2 (%)	8.230	7.520	7.140	6.260	8.340	7.560	7.170	6.570
f_3 (%)	1.560	1.330	1.260	1.010	1.630	1.340	1.270	1.140
n_{HB}	580.67	537.14	514.11	485.63	584.43	545.16	518.18	495.33

Table 5 Average lifetime of hydrogen bonds (τ) with a different number of Mg^{2+} ions (nM) added

	Without an electrostatic field				Under an electrostatic field			
	0M	1M	2M	3M	0M	1M	2M	3M
τ (ps)	52.06	53.18	54.27	55.99	52.21	53.23	54.54	56.37

Table 6 Average radii of the first water shell of Ca^{2+} and first water coordination number of Ca^{2+} under the electrostatic field with different numbers of Mg^{2+} ions added

	Without an electrostatic field				Under an electrostatic field			
	0M	1M	2M	3M	0M	1M	2M	3M
R_{Ca-O} (nm)	0.282	0.282	0.280	0.282	0.278	0.280	0.276	0.280
n_{Ca-O}	5.62	5.30	5.07	5.00	5.70	5.41	5.22	4.90

dynamical residence time of water molecules around Ca^{2+} is because of the change in the diffusion coefficient of water molecules. When Mg^{2+} ions are added to the calcium chloride

solution, the electrostatic interaction between Mg^{2+} and water molecules makes the diffusion coefficient of water molecules decrease, which causes the water molecules around Ca^{2+} to move in and out of the first shell less frequently.³⁷ According to Table 3, the electrostatic field can make the mean dynamical residence time of water molecules around Ca^{2+} in the four representative $CaCl_2$ aqueous solutions decrease. This is because the activity of water molecules is enhanced by the electrostatic field, which makes the water molecules around Ca^{2+} move in and out of the first shell much more frequently. Therefore the mean dynamical residence time of water around Ca^{2+} decreased.

3.3 Viscosity of the $CaCl_2$ aqueous solution

The dynamic viscosity of a liquid is a kinetic property that influences the rates of conformational changes of solutes in the liquid. It can be influenced by an electrostatic field.³⁸ The viscosity (η) can be calculated using the following equation:

$$\eta = \frac{A}{V} \frac{\rho}{k^2} \quad (4)$$

where ρ and V are the density and velocity, respectively; A is a constant³⁸ and from a cosine that satisfies both conditions:

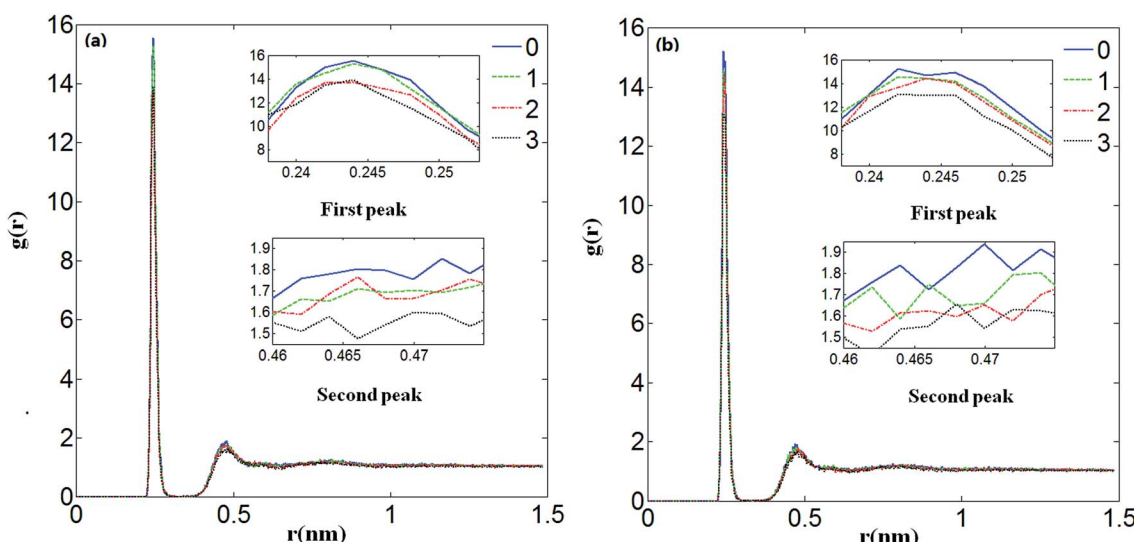


Fig. 6 Effects of Mg^{2+} ions on $g(r)$ ion–water in the $CaCl_2$ aqueous solution system with no Mg^{2+} ions added (solid line), ten Mg^{2+} ions added (dashed line), twenty Mg^{2+} ions added (dash-dotted line) and thirty Mg^{2+} ions added (dotted line) under no electrostatic field (a) and under the electrostatic field (b).



$$a_x = A \cos(kz), k = 2\pi/l_z \quad (5)$$

where l_z is the height of the box. We define the instantaneous V in the simulation as a Fourier coefficient:

$$V(t) = \frac{2 \sum_{i=1}^N m_i v_{i,x}(t) \cos[kr_{i,z}(t)]}{\sum_{i=1}^N m_i} \quad (6)$$

where $v_{i,x}$ is the x component of the velocity; $r_{i,z}$ is the z coordinate; m_i is the mass of an atom. The average of V can be measured after the amplitude of the velocity profile has been fully developed.

Fig. 2 shows the viscosity of four representative CaCl_2 aqueous solutions under an electrostatic field. The values under no electrostatic field are presented for comparison. From Fig. 2, it can be found that the viscosity of the four representative CaCl_2 aqueous solutions increases under the action of Mg^{2+} , and there is a positive correlation between the viscosity value and the number of Mg^{2+} ions added in the CaCl_2 systems. In addition, the electrostatic field can make the viscosity of CaCl_2 aqueous solutions smaller without the addition of Mg^{2+} ions. But the electrostatic field can make the viscosity of CaCl_2 aqueous solutions increase when a certain amount of Mg^{2+} ions is added to the CaCl_2 aqueous solutions.

The dynamic viscosity can be described as a type of friction caused by the fluid's motion inside the solution system. Its value is proportional to the number of carbon–hydrogen bonds and the particles' molecular weight in the solution system. It should be realized that the viscosity is a macroscopic property that represents the average behaviour of a large number of water molecules in aqueous solution.³² Therefore, the change in dynamic viscosity can be attributed to the changes in the structural and dynamics parameters of water molecules. Baker³² found that the large influence of some ions on the viscosity of water is due to the long lifetime of their first hydration shells using molecular dynamics simulations. The longer residence times of the water molecules in ion hydration shells strongly increases the viscosity. Since CaCl_2 is an inorganic salt in an aqueous solution, there is no carbon–hydrogen bond in it. Therefore, the decrease in the viscosity of the CaCl_2 solution should only be attributed to the changes in the structural change and dynamics parameters of water molecules. Combined with Fig. 2, the addition of Mg^{2+} forms a water shell which can result in a long residence time of water molecules in the Mg^{2+} hydration shells. Moreover, the addition of Mg^{2+} makes the mean dynamical residence time of water around Ca^{2+} increase as discussed earlier, which can also increase the viscosity of the CaCl_2 aqueous solutions. This result can also match with the data in Fig. 1. The activity of water molecules is related to the viscosity of the solution. According to Fig. 1, the activity of water molecules is more limited when more Mg^{2+} ions are added, and this can make the viscosity of the solution increase. The results in Fig. 2, show that the electrostatic field can make the viscosity of CaCl_2 aqueous solutions decrease without the addition of Mg^{2+} ions. The electrostatic field

increases the activity of water molecules and decreases the mean dynamical residence time of water around Ca^{2+} , which causes a decrease in the dynamic viscosity. In the case of the CaCl_2 solution containing Mg^{2+} , although the electrostatic field increases the activity of water molecules that can result in the viscosity decrease, the Mg^{2+} has a stronger binding ability with water molecules than Ca^{2+} due to the smaller effective radius³⁷ and the longer lifetime of water molecules around Mg^{2+} .³² This means that Mg^{2+} has a stronger ability to increase the viscosity of the solution than Ca^{2+} . The electrostatic interaction between Mg^{2+} ions and water molecules can make the viscosity of the solution increase. This ability is stronger than the ability of the electrostatic field to decrease the viscosity of the solution, which causes an increase in the dynamic viscosity of the CaCl_2 solution. To sum up, a certain amount of Mg^{2+} can increase the viscosity of the CaCl_2 aqueous solution, and when the electrostatic field is applied to the CaCl_2 solution containing Mg^{2+} , the viscosity of the CaCl_2 aqueous solution can also be increased.

3.4 Effects of Mg^{2+} ions and electrostatic fields on hydrogen bonds

3.4.1 Structure and number of hydrogen bonds. The characteristics of hydrogen bonds are directly related to the physical and chemical properties of the aqueous solution.^{39,40} In the Gromacs software, the hydrogen bond is defined as the distance from a donor to an acceptor, which is less than the van der Waals (VDW) distance of 3.5 Å (r) and the angle of the hydrogen–donor–acceptor is smaller than 30°.⁴¹ Fig. 3 shows the geometrical hydrogen bond criterion. In the present study receptors and donors are oxygen atoms in water molecules. The hydrogen bond angle calculated in this study is $\angle \text{H}_D\text{--O}_D\text{--O}_A(\theta)$ which is a useful angle often used in the literature that provides valuable insight into the flexibility of donor hydrogen bonds.⁴² When a molecule forms hydrogen bonds with another molecule, the overall hydrogen bonding potential of the molecule becomes larger. However, the angle variation will change the distance between atoms and the Coulomb force and van der Waals (VDW) force will also change, which influences the stability of hydrogen bonds. A hydrogen bond can be broken by an increase of water rotation (increasing θ).⁴²

Fig. 4 shows the distribution of the hydrogen bond angle θ under the electrostatic field and the value under no electrostatic field is presented for comparison. Fig. 5 shows the distributions of the hydrogen bond angle θ under no electrostatic field and under the electrostatic field with different numbers of Mg^{2+} ions added, respectively. For clarification, the peaks are enlarged in the small figures. The distributions of the hydrogen bond angle θ shown in Fig. 4 and Fig. 5 are Poisson distributions, which are similar to those obtained from other simulations.^{42,43}

It can be seen in Fig. 5(a) that under no electrostatic field the peak coordinates of the distribution of the hydrogen bond angle θ are (11.5, 0.0560083), (9.5, 0.0569745), (8.5, 0.0562455) and (9.5, 0.0588264) when 0 Mg^{2+} ions, ten Mg^{2+} ions, twenty Mg^{2+} ions, and thirty Mg^{2+} ions are added, respectively. According to Fig. 5(b), when 0 Mg^{2+} ions, ten Mg^{2+} ions, twenty Mg^{2+} ions, and thirty Mg^{2+} ions are added, respectively, under an



electrostatic field, the peak coordinates of the distribution of the hydrogen bond angle θ are (9.5, 0.0585088), (8.5, 0.0585088), (8.5, 0.0592885) and (7.5, 0.0558013). It is shown in Fig. 5(a) and (b) that the positions of the statistical curve peaks all shift to smaller angles. The heights of the peaks all rise with the increase in the number of added Mg^{2+} ions and the application of an electrostatic field. Both the electrostatic field and Mg^{2+} ions can change the distribution of the hydrogen bond angle and make the average hydrogen bond angle smaller. It means that the Mg^{2+} and the electrostatic field can enhance the hydrogen bonding between water molecules to a certain extent.

In the present study the number of hydrogen bonds (n_{HB}) and the percentage of water molecules with n hydrogen bonds (f_n) are also investigated. The f_n and n_{HB} in $CaCl_2$ aqueous solutions without Mg^{2+} ions added (0M), with ten Mg^{2+} ions added (1M), with twenty Mg^{2+} ions added (2M) and with thirty Mg^{2+} ions added (3M) are listed in Table 4. In addition, the influence of the electrostatic field is also presented.

According to Table 4, the electrostatic field can decrease the fraction of molecules having no hydrogen bonds, while it can increase the fraction of molecules having one to three hydrogen bonds and the average number of hydrogen bonds per water molecule whether Mg^{2+} is added or not. The reduction of f_0 and the increase of n_{HB} , f_1 , f_2 , and f_3 show that the activity of water molecules is restrained and more water molecules shift from a free state to a hydrogen-bonded state, which means that the hydrogen bonding of water molecules was enhanced by the electrostatic field. The results in Table 4 also show that the Mg^{2+} ions can increase f_0 and decrease n_{HB} , f_1 , f_2 , and f_3 whether the electrostatic field is applied or not. Furthermore, f_0 increases with the increase in the number of Mg^{2+} ions added, and n_{HB} , f_1 , f_2 , and f_3 decrease with the increase in the number of Mg^{2+} ions added to the $CaCl_2$ systems.

The electrostatic field of ions can influence the hydrogen bond structure when water molecules are in the vicinity of cations that do not form any hydrogen bonds. The water molecules in the cation hydration shells are also held through ion-dipole interactions.⁴⁴ When the cation is present, more non hydrogen-bonded water molecules stay in the ion hydration shell due to attractive ion-dipole interactions. The number of water molecules bound by hydrogen bonding decreases. Then a smaller number of hydrogen bonds are formed, the fraction of molecules having no hydrogen bonds increases, and the fraction of molecules having one to three hydrogen bonds and the average number of hydrogen bonds per water molecule decrease.

3.4.2 Hydrogen bond lifetime. Hydrogen bond strength can be evaluated by calculating the lifetime of hydrogen bonds. It is a positive correlation between the lifetime of hydrogen bonds and the hydrogen bond strength.⁴¹ Since the water molecules are in rapid vibration, the hydrogen-bonded water molecules break at a certain time and then form hydrogen bonds with other water molecules.⁴⁵ The hydrogen bond lifetime is a parameter that measures the different hydrogen bond lifetimes in different states throughout the dynamic process.

The lifetime of hydrogen bonds (τ_{HB}) can be calculated using eqn (7):²¹

$$\tau_{HB} = \int_0^\infty C(\tau) d\tau \quad (7)$$

where $C(\tau)$ is the hydrogen bond correlation function. The $C(\tau)$ is defined as:

$$C(\tau) = \langle h_i(t)h_i(t + \tau) \rangle \quad (8)$$

where $h_i(t) = \{0, 1\}$ is the Heaviside unit step function, and it means that if two molecules formed hydrogen bonds at time 0 and t , the function value is 1, and otherwise 0.

According to Table 5, the electrostatic field increases the average lifetime of the hydrogen bond whether Mg^{2+} is added or not. The increase of τ due to the hydrogen bonding of water molecules is enhanced by the electrostatic field as discussed earlier. In addition, the results in Table 5 show that the Mg^{2+} ions can increase the average lifetime of the hydrogen bond. The hydrogen bond formed in the cationic water shell is relatively strong.⁴⁶ Therefore, the addition of Mg^{2+} can cause more water shells to form with water molecules which increases the average lifetime of the hydrogen bond.

3.5 Structure parameters

In this section, the average radii of the first water shell of Ca^{2+} ions (R_{Ca-O}), the first coordination numbers of Ca^{2+} (n_{Ca-O}) and the RDF (radial distribution function) of Ca^{2+} and water molecules are discussed under the addition of Mg^{2+} ions, the external electrostatic field and no electrostatic field, respectively. R_{Ca-O} can be obtained from the radial distribution function [$g(r)$]. The form of [$g(r)$]⁴⁷ is shown in eqn (9):

$$g_{AB}(r) = \frac{\langle \rho_B(r) \rangle}{\langle \rho_B(r) \rangle_{local}} = \frac{1}{\langle \rho_B(r) \rangle_{local}} \frac{1}{N_A} \sum_{i \in A}^{N_A} \sum_{j \in B}^{N_B} \frac{\delta(r_{ij} - r)}{4\pi r^2} \quad (9)$$

where N_A is the quantity of particle A, and N_B is the quantity of particle B; $\langle \rho_B(r) \rangle$ is the particle density of particle B at a distance r from particle A, and $\langle \rho_B(r) \rangle_{local}$ is the particle density of particle B averaged over all spheres around particle A with radius r_{max} . Usually the value of r_{max} is half of the minimum box length.

The value of n_{Ca-O} is calculated using eqn (10)¹⁹

$$n_{Ca}^0(r_s) = 4\pi\rho_0 \int_0^{r_s} g_{CaO}(r) r^2 dr \quad (10)$$

For n_{Ca-O} , r_s is the location of the first local minimum of $g_{CaO}(r)$.

Table 6 presents the effect of Mg^{2+} ions on the average radii of the first water shell for Ca^{2+} and the first water coordination number of Ca^{2+} . The standard deviation of R_{Ca-O} is between 0.0014 nm and 0.0016 nm, and the standard deviation of n_{Ca-O} is between 0.024 and 0.030. The results in Table 5 show that the electrostatic field can make the radii of the first water shell of Ca^{2+} smaller.

According to Table 6, the addition of Mg^{2+} had no significant effect on R_{Ca-O} . Meanwhile, Table 5 shows that n_{Ca-O} decreases with the increase in the number of Mg^{2+} ions added. The hydration between Mg^{2+} ions and water molecules is stronger



than the hydration between Ca^{2+} and water molecules, which means the existence of Mg^{2+} ions can make fewer water molecule stay in the water shell of Ca^{2+} . The addition of Mg^{2+} ions has no obvious effect on $R_{\text{Ca-O}}$, but decreases $n_{\text{Ca-O}}$.

The RDFs of Ca^{2+} and water molecules with different numbers of Mg^{2+} ions added under no electrostatic field (a) and under the electrostatic field (b) are presented in Fig. 6. It shows the effects of Mg^{2+} ions on $g_{\text{Ca-water}}(r)$. It can be seen that the first and second peaks decrease with the increase in the number of Mg^{2+} ions added, which means the addition of Mg^{2+} ions weakens the interaction between Ca^{2+} and water molecules. It matches the previous conclusion that Mg^{2+} weakens the interaction between Ca^{2+} and water molecules due to the Mg^{2+} ions binding more strongly than Ca^{2+} to water molecules.

According to Table 6, compared with the structure parameters under no electrostatic field, the values of $R_{\text{Ca-O}}$ are smaller and the values of $n_{\text{Ca-O}}$ are larger under the electrostatic field, which means that an electrostatic field can not only make the Ca^{2+} ions and water molecules gather more compactly but it can also increase the number of coordinated water molecules when no, ten or twenty Mg^{2+} ions are added in it. Therefore when there is an electrostatic field, the decrease of $R_{\text{Ca-O}}$ and the increase of $n_{\text{Ca-O}}$ all can be attributed to the enhanced hydration between Ca^{2+} ions and water molecules. The enhanced electrostatic interaction not only causes the hydrated water molecules to be closer to Ca^{2+} but also attracts more water molecules as coordinated water molecules. The increase of the first water coordination number of Ca^{2+} ions enhances their inhibition to carbonate ions, which shows that the electrostatic field decreases the formation probability of the calcium carbonate precipitate.

4 Conclusions

The influences of Mg^{2+} ions and the electrostatic field on CaCl_2 aqueous solutions were studied. The effects of different numbers of Mg^{2+} ions were compared and the anti-fouling performance under the influence of an electrostatic field and under no electrostatic field was compared, and the structural changes and dynamic properties of CaCl_2 aqueous solutions under the electrostatic field were researched by a systematic long-time, equilibrium molecular dynamics simulation. Some important conclusions were obtained.

The electrostatic field decreases the mobility of the Ca^{2+} ions when Mg^{2+} ions are added. The impurity Mg^{2+} ions can effectively increase the viscosity of the CaCl_2 aqueous solution and decrease the self-diffusion coefficient of particles by the electrostatic interaction between Mg^{2+} ions and water molecules. The more Mg^{2+} ions are added, the bigger the viscosity of the CaCl_2 aqueous solution is, and the lower the diffusion coefficient of the particles is. Therefore, the presence of Mg^{2+} ions can decrease the rate of the chemical reaction between Ca^{2+} and CO_3^{2-} ions by decreasing the activity of ions.

The addition of Mg^{2+} ions can make the average hydrogen bond angle smaller and increase the average lifetime of hydrogen bonds. The addition of Mg^{2+} ions can also increase the mean dynamical residence time of water around Ca^{2+} ions.

The more Mg^{2+} ions are added, the bigger the average lifetime of hydrogen bonds is, and the bigger the mean dynamical residence time of water around Ca^{2+} ions is. The electrostatic field enhances the hydrogen bonding between water molecules which reflects in the decrease of the average hydrogen bond angles, the increase in the number of hydrogen bonds, and the average lifetime of hydrogen bonds.

Electrostatic fields can decrease the radii of the first water shell of hydrated Ca^{2+} ions. Under the action of an electrostatic field, regardless of whether or not Mg^{2+} ions exist, the ratio of free water molecules in the calcium chloride solution decreased and the binding force of the hydrated calcium ions to the surrounding water molecule is enhanced.

Conflicts of interest

There are no conflicts of interest to declare.

Acknowledgements

This work was financially supported by the National Natural Science Foundation of China (Grant No. 51408525 and 51608468).

References

- 1 J. Q. Qi, R. Guo and Y. Wang, *Nanoscale Res. Lett.*, 2016, **11**, 120.
- 2 L. I. Haihua, Z. F. Liu and Y. H. Gao, *CIESC J.*, 2013, **64**, 1736.
- 3 M. Kitamura, *J. Colloid Interface Sci.*, 2001, **236**, 318–327.
- 4 A. Gutjahr, H. Dabringhaus and R. Lacmann, *J. Cryst. Growth*, 1996, **158**, 310–315.
- 5 N. H. DeLeeuw, *J. Phys. Chem. B*, 2002, **106**, 5241–5249.
- 6 G. J. Zhao, J. Y. Liu and L. C. Zhou, *J. Phys. Chem. B*, 2007, **111**, 8940–8945.
- 7 G. J. Zhao and K. L. Han, *Acc. Chem. Res.*, 2012, **45**, 404.
- 8 J. S. Chen, M. H. Yuan and J. P. Wang, *J. Phys. Chem. A*, 2014, **118**, 8986.
- 9 P. L. De and M. L. Chávez, *Langmuir*, 2005, **21**, 10874–10884.
- 10 Y. I. Cho and R. Liu, *Int. J. Heat Mass Transfer*, 1999, **42**, 3037–3046.
- 11 X. Xiaokai, M. Chongfang and C. Yongchang, *Chem. Eng. Technol.*, 2010, **28**, 1540–1545.
- 12 J. Wang, X. Feng and W. Du, *Mol. Phys.*, 2008, **106**, 2685–2697.
- 13 X. K. Xing, C. F. Ma and Y. C. Chen, *Chem. Eng. Technol.*, 2010, **28**, 1540.
- 14 N. A. Hewish, G. W. Neilson and J. E. Enderby, *Nature*, 1982, **297**, 138–139.
- 15 J. L. Fulton, Y. Chen and S. M. Heald, *J. Phys. Chem. A*, 2006, **125**, 431.
- 16 G. Licheri, G. Piccaluga and G. Pinna, *J. Phys. Chem.*, 1976, **64**, 2437.
- 17 M. Zhang, C. Li and M. Benjamin, *Environ. Sci. Technol.*, 2003, **37**(8), 1663–1669.
- 18 M. Nedyalkova, S. Madurga and S. Pisov, *J. Chem. Phys.*, 2012, **137**, 1.



19 A. A. Chialvo and J. M. Simonson, *J. Chem. Phys.*, 2003, **119**, 8052–8061.

20 R. E. IseleHolder, W. Mitchell and A. E. Ismail, *J. Chem. Phys.*, 2012, **137**, 1133.

21 W. F. V. Gunsteren, *Biomolecular Simulation: the GROMOS96 Manual and User Guide*, Zürich, Groningen, 1996.

22 Y. Han and Y. Zhao, *Int. J. Electrochem. Sci.*, 2012, **7**, 10008–10026.

23 S. Tsuzuki, W. Shinoda and H. Saito, *J. Phys. Chem. B*, 2009, **113**, 10641–10649.

24 P. Henritzi, A. Bormuth and F. Klameth, *J. Chem. Phys.*, 2015, **143**, 164502.

25 M. A. Fischler and R. C. Bolles, *Commun. ACM*, 1981, **24**, 381.

26 Y. Han, L. Zhu and Y. Zhang, *Chem. Res. Chin. Univ.*, 2016, **32**, 1–6.

27 B. Guo, H. B. Han and F. Chai, *Trans. Nonferrous Met. Soc. China*, 2011, **21**, s494–s498.

28 F. C. Lightstone, E. Schwegler and R. Q. Hood, *Chem. Phys. Lett.*, 2001, **343**, 549–555.

29 M. Rybicki and E. Hawlicka, *Chem. Phys.*, 2012, **400**, 79–85.

30 J. Dian, K. Christopher and G. Alan, *J. Phys. Chem. B*, 2006, **110**, 18553.

31 S. Wei, C. Zhong and H. SuYi, *Mol. Simul.*, 2005, **31**, 555–559.

32 H. J. Bakker, *Chem. Rev.*, 2008, **108**, 1456.

33 Y. Zhu, L. Xiaohua and D. Hao, *Mol. Simul.*, 2003, **29**, 767–772.

34 M. J. Wei, L. Zhang and L. Lu, *Phys. Chem. Chem. Phys.*, 2012, **14**, 16536–16543.

35 M. M. Naor, K. V. Nostrand and C. Dellago, *Chem. Phys. Lett.*, 2003, **369**, 159–164.

36 C. F. Schwenk, H. H. Loeffler and B. M. Rode, *Chem. Phys. Lett.*, 2001, **349**, 99–103.

37 D. Jiao, C. King and A. Grossfield, *J. Phys. Chem. B*, 2006, **110**, 18553.

38 B. Hess, *J. Chem. Phys.*, 2002, **116**, 209–217.

39 W. J. Lee, J. G. Chang and S. P. Ju, *Langmuir*, 2010, **26**, 12640–12647.

40 Z. Pan, J. Chen and L. Gang, *J. Chem. Phys.*, 2012, **136**, 164313.

41 X. Zhang, Q. Zhang and D. X. Zhao, *Acta Phys.-Chim. Sin.*, 2011, **27**, 2547.

42 H. S. Lee and M. E. Tuckerman, *J. Chem. Phys.*, 2006, **125**, 154507.

43 K. Modig, B. G. Pfrommer and B. Halle, *Phys. Rev. Lett.*, 2003, **90**, 075502.

44 A. Karmakar, J. R. Choudhuri and V. K. Yadav, *Chem. Phys.*, 2013, **412**, 13–21.

45 A. Luzar and D. Chandler, *Nature*, 1996, **379**, 55–57.

46 E. Guàrdia, J. Martí and L. García-Tarrés, *J. Mol. Liq.*, 2005, **117**, 63–67.

47 D. M. York, T. A. Darden and L. G. Pedersen, *J. Chem. Phys.*, 1993, **32**, 1443–1453.

